JOURNAL OF COMPUTATIONAL PHYSICS 104, 451–456 (1993)

On the Numerical Accuracy of the Fokker–Planck Approximation to the Hierarchy of Master Equations

C. A. STONE, M. VICANEK, AND N. M. GHONIEM

Mechanical, Aerospace and Nuclear Engineering Department, UCLA, Los Angeles, California 90024

Received May 9, 1991; revised May 6, 1992

Many physical processes are described by birth and death phenomena and can generally be treated with either a master equation or Fokker–Planck formulation. We present a numerical study for one such process which describes the agglomeration of atomic clusters on clean surfaces during the early stages of thin film formation. We develop moment equations which describe the evolving size distribution of these clusters during an atom deposition process. These moments are derived from both the hierarchical master equations and the equivalent Fokker–Planck approximation. We limit our treatment to growth and decay mechanisms which occur via single-atom transitions. It is shown that the Fokker–Planck approximation is surprisingly good for sizes down to a few atoms. Analysis of the numerical accuracy of the Fokker–Planck approximation is given by comparing results for the total density of clusters, their average size, and the first four moments of the size distribution function. Results are presented for growth laws associated with two- and three-dimensional cluster shapes.

1. INTRODUCTION

In many applied branches of nonequilibrium statistical physics, several levels of models can be constructed for the description of the same phenomenon. The beauty of statistical mechanics, which describes the interactions between a large ensemble of similar entities, manifests itself in the self-consistency in which different types of models characterize the same phenomenon. The premise of such an approach is that, once a deterministic law is prescribed for the interaction of similar entities, one should be able to determine global and experimentally verifiable phenomenological parameters, regardless of the level of model used.

This approach of statistical mechanics is indeed a cornerstone in advances made in all areas of physics which are based on single-particle behavior. Primary applications of this approach are embodied in the kinetic theory of gases, as well as extensions to plasma physics, neutron transport, and radiation transport. When applied to such fields, statistical mechanics leads to global conservation equations (e.g., Navier–Stokes, diffusion, or Boltzmann transport equations). The connection between such macroscopic "fluid" models and the corresponding microscopic "particle" models is maintained through coefficients which arise in the macroscopic conservation equations. These coefficients can be calculated in terms of single-particle mechanics.

A specific application of this procedure can be found in phenomena which are governed by birth and death processes [1]. These macroscopic processes are representative of the fundamental laws of statistical mechanics at the single-particle level. Such processes have often been used to describe chemical reactions [2], the population ecology of social insect colonies [3], and vehicular traffic systems [4], although initial applications appeared around the turn of the century, notably in the works of Smoluchowski [5], Chapman [6], and Kolmogoroff [7]. The transitions (or birth and death processes) between different states of the system are modeled by an infinite set of hierarchical master equations (MEs). When the transition size is small in comparison to the size of the state at which the transition is occuring, an approximate conservation equation can be derived. This approximation is the well-known Fokker–Planck (FP) equation [8]. One notable and early example of this approximation was presented by Chandrasekhar [9] who studied the coagulation of colloid particles, obtaining analytical expressions for the colloid size distribution as a function of time.

Langevin equations are sometimes used to describe single-particle motion with a fluctuating force component [9]. This description is similar to the problem of Brownian motion in a deterministic force field. It can be shown [9] that this description can be reduced to the Fokker–Planck formulation. It is generally discussed that the FP approximation is some sort of "thermodynamic limit" to the hierarchy of MEs. Nicolis and Prigogine [1] argue that this limit is asymptotically realized either in the limit of long times or if a large number of particles are in the system.

A generic master equation, which represents the time rate of change in the probability of a given hierarchical state of the system, is transformed to a Fokker–Planck equation via

0021-9991/93 $5.00

the Kramers–Moyal expansion [10, 11]. In this approach, terms of $O(\Delta^3)$ are ignored, where Δ is the relative transition size.

A problem of current interest, which is generally modeled by master, Fokker–Planck, or Langevin-type equations, is the agglomeration of atoms into small atomic clusters. This problem emerges in several areas, such as radiation effects [12, 13] and thin film nucleation [14, 15, 16, 17]. Various numerical schemes have been proposed for the solution of either master or Fokker–Planck equations. Since direct solutions of the hierarchy of equations which represent atomic clusters is computationally intractable for clusters containing thousands of atoms, approximate numerical methods are desired. Examples are finite difference [18], finite solution-space [19], grouping [20, 21], propagator [16], and moments [17, 22] methods.

A successful description of atomic clustering phenomena must couple the nucleation and growth phases of the process. This complete description can be achieved directly by solving the characteristic master equations. The equivalent Fokker–Planck approximation, however, accounts for nucleation and growth via appropriate boundary conditions. For this purpose, we developed a two-group approach for the description of particle cluster aggregation [23]. We have also developed a moments solution to the Fokker–Planck equation describing interstitial loops in irradiated materials [22] and surface clusters during thin film formation [17]. While the moments approach is computationally superior to finite-grid-type numerical techniques, it has the additional advantage of giving direct physical insight into atomic clustering physics. Comparisons with experimentally determined moments can reveal features of fundamental atomic clustering mechanisms.

In this paper, we wish to compare the accuracy of numerical moment solutions using both a master equation formulation [23, 24] and a Fokker–Planck approximation [17, 25]. For this purpose and for self-consistency, it is necessary to briefly outline the two methods in Section 2. A comparison of cluster densities, average size, and various moments of the size distribution is presented in Section 3. Our conclusions from these comparisons are summarized in Section 4.

2. PROBLEM FORMULATION

In the present formulation, we assume that thermal atoms are deposited on an atomically clean, smooth surface, and that only single atoms are mobile. We also assume that the dissociation rate of clusters containing two or more atoms is negligible, compared to the aggregation rate. Single atoms can aggregate with i-atom clusters at the rate of $W(1, i)$ $C(1, t)$ $C(i, t)$, where $W(1, i)$ is a size-dependent rate constant. $C(1, t)$ denotes the density of mobile single atoms present on the surface at time t, whereas $C(i, t)$ is the density of i-atom clusters. Single atoms can also evaporate off the surface at the rate of $v_a C(1, t)$, where v_a is the evaporation frequency. Letting q represent the deposition rate of mobile single atoms, then the birth and death equations describing this simple clustering system are given by

$$\frac{\partial C(1, t)}{\partial t} = q - v_a C(1, t) - 2W(1, 1)\, C^2(1, t) - \sum_{i=2}^{\infty} W(1, i)\, C(1, t)\, C(i, t) \tag{1}$$

$$\frac{\partial C(i, t)}{\partial t} = W(1, i-1)\, C(1, t)\, C(i-1, t) - W(1, i)\, C(1, t)\, C(i, t), \qquad i \geqslant 2. \tag{2}$$

The factor of 2 in the $-2W(1, 1)\, C^2(1, t)$ term of Eq. (1) accounts for the fact that *two* single atoms are lost in the production of a two-atom cluster. This simple system is similar to the one developed by Zinsmeister [14, 26] and used by Adams and Hitchon [16]. The effects of mobility coalescence [23], cluster dissociation [17], and atom trapping at surface defects [17] have been previously analyzed. In the present work, however, we wish to make the comparison clear by focusing only on deposition, evaporation, and single-atom aggregation phenomena. In this respect, the comparison between the ME and FP approaches is based on a minimum number of physically realizable processes. Furthermore, the aggregation rate constant, $W(1, i)$, is assumed to have the size dependence

$$W(1, i) = W_0(1 + i^r), \tag{3}$$

where the growth exponent, r, equals $\frac{1}{2}$ for 2D cluster growth, and $\frac{1}{3}$ for 3D clusters. For a comprehensive discussion of the clustering model, the reader is referred to our previous work [17, 27].

2.1. *Direct Moment Equations*

Introduce power moments, $N_k(t)$, of the cluster size distribution according to

$$N_k(t) = \sum_{i=1}^{\infty} i^k C(i, t). \tag{4}$$

The total cluster density is denoted by $N_0(t)$, while $N_1(t)$ represents the total number of atoms, per unit surface area.

Taking the time derivative of Eq. (4), we use Eq. (1) and (2) to obtain

$$\frac{\partial N_k(t)}{\partial t} = q - v_a C(1, t) + \sum_{i=1}^{\infty} W(1, i)\, C(1, t)\, C(i, t) \times [(i+1)^k - i^k - 1]. \quad (5)$$

The clusters are now classified into two size groups, $i < X_c$ and $i \geqslant X_c$. A continuous description is used for large clusters, where $C(x, t)$ is used instead of $C(i, t)$, and sums are replaced by integrals. The transition cluster size, X_c, is defined as the smallest size described by the continuum. It should be noted that $X_c \geqslant 2$. We now introduce the moments, $M_k(t)$, of the large cluster population as

$$M_k(t) = \int_{X_c}^{\infty} x^k C(x, t)\, dx \quad (6)$$

such that $M_k(t)$ and $N_k(t)$ are related by

$$M_k(t) = N_k(t) - \sum_{i=1}^{X_c - 1} i^k C(i, t). \quad (7)$$

To obtain a set of closed moment equations for $M_k(t)$, we expand all size-dependent quantities in a second-order Taylor series evaluated at the average continuum-cluster size, $\bar{x}(t) = M_1(t)/M_0(t)$. Solving this set of kinetic moment equations yields the solution to the corresponding ME problem. The moments of the large-size cluster population, $M_k(t)$, can then be used to determine characteristics of the continuum-cluster size distribution, as shown in Table I. Details of this procedure are given in Ref. [23] and therefore will not be reproduced here.

2.2. *Fokker–Planck Approximation*

Consider Eq. (2), where the cluster density, $C(i-1, t)$, and the rate constant, $W(1, i-1)$, are both expanded in a second-order Taylor series about i. This procedure is standard in birth and death formulations and yields the following approximation for $x \geqslant 2$ which has the form of a Fokker–Planck equation:

$$\frac{\partial C(x, t)}{\partial t} = -\frac{\partial}{\partial x}\left\{\mathscr{F}(x, t)\, C(x, t) - \frac{\partial}{\partial x}[\mathscr{D}(x, t)\, C(x, t)]\right\} \quad (8)$$

where the drift and dispersion frequency functions, $\mathscr{F}(x, t)$ and $\mathscr{D}(x, t)$, are given by

$$\mathscr{F}(x, t) = W(1, x)\, C(1, t) \quad (9)$$

$$\mathscr{D}(x, t) = \tfrac{1}{2}\mathscr{F}(x, t), \quad (10)$$

where the continuous variable, x, has replaced the discrete variable, i, for the cluster size. A general discussion of the master and FP equations is given by Reif [28].

Equation (8) can be used to develop kinetic moment equations for the following characteristics of the large-size cluster population: $C_{\text{tot}}(t)$, the total density of continuum clusters,

$$C_{\text{tot}}(t) = \int_{X_c}^{\infty} C(x, t)\, dx; \quad (11)$$

$\langle x \rangle(t)$, the average size of continuum clusters,

$$\langle x \rangle(t) = \left(\frac{1}{C_{\text{tot}}(t)}\right) \int_{X_c}^{\infty} x C(x, t)\, dx; \quad (12)$$

and $\mathscr{M}_n(t)$, the nth central moment of the continuum-cluster size distribution,

$$\mathscr{M}_n(t) = \left(\frac{1}{C_{\text{tot}}(t)}\right) \int_{X_c}^{\infty} [x - \langle x \rangle(t)]^n\, C(x, t)\, dx. \quad (13)$$

The procedure then remains to solve a set of discrete kinetic rate equations for the small-size cluster population [i.e., Eqs. (1) and (2) for cluster sizes up to $i = (X_c - 1)$] which

TABLE I

Characteristics of the Continuum-Cluster Size Distribution, $x \geqslant X_c$, Based on a Master Equation (ME) Solution

Characteristic	ME notation
Total cluster density [#/cm^2]	$M_0(t)$
Average cluster size [atoms]	$M_1(t)/M_0(t) \equiv \bar{x}(t)$
Second scaled moment	$M_2(t)/\bar{x}^2(t)$
Third scaled moment	$M_3(t)/\bar{x}^3(t)$
Fourth scaled moment	$M_4(t)/\bar{x}^4(t)$

TABLE II

Characteristics of the Continuum-Cluster Size Distribution, $x \geqslant X_c$, Based on a Fokker–Planck (FP) Solution

Characteristic	FP notation
Total cluster density [#/cm^2]	$C_{\text{tot}}(t)$
Average cluster size [atoms]	$\langle x \rangle(t)$
Second scaled moment	$\mathscr{M}_2(t)/\langle x \rangle^2(t)$
Third scaled moment	$\mathscr{M}_3(t)/\langle x \rangle^3(t)$
Fourth scaled moment	$\mathscr{M}_4(t)/\langle x \rangle^4(t)$

are coupled to kinetic moment equations for $C_{tot}(t)$, $\langle x \rangle(t)$, and $\mathcal{M}_n(t)$. This procedure, together with the appropriate initial and boundary conditions, has been discussed in Refs. [17, 27] and thus will not be repeated here. The resulting FP solution can be used to determine characteristics of the continuum-cluster size distribution, as shown in Table II.

3. COMPARISON OF THE ME AND FP NUMERICAL SOLUTIONS

Developing moments directly from the master equation, or an equivalent moment formulation from the Fokker–Planck approximation, results in a stiff system of coupled, non-linear, ordinary differential equations which couple discrete, small-size clusters to a continuum, large-size population. Solving this system of equations yields quantities which are characteristic of the complete cluster distribution. These quantities are the densities of the small-size clusters for sizes up to $(X_c - 1)$, as well as quantities which are characteristic of the large-size "continuum" population (specifically, the total density of continuum clusters, the average size of continuum clusters, and higher moments of the continuum cluster distribution function). In this section, we present a comparison between the ME and FP solution techniques for various values of the transition cluster size, X_c, and the growth exponent, r.

In both the ME and FP solutions, thermal particle deposition is assumed to begin on a bare, defect-free substrate at time zero. Single atoms are deposited at a rate of $q = 10^{13}$ atoms/cm^2/s, and mobile single atoms evaporate off the substrate at a frequency of $\nu_a = 2.74 \times 10^5\ \mathrm{s}^{-1}$. The aggregation rate coefficient is taken to be $W_0 = 1.50 \times 10^{-5}$ cm^2/s. It should be noted that ν_a and W_0 depend on such physical system properties as the substrate temperature and lattice parameter, activation energies for adatom desorption and diffusion, characteristic vibrational frequencies, and the size of the deposited atoms; however, the above values are used for this study.

To investigate the accuracy of the FP approximation to the corresponding ME solution, features of the large-size, "continuum" cluster population will be compared. These characteristics, which include the total cluster density, average cluster size, and various moments of the continuum-cluster size distribution, are listed in Tables I and II for both solution methods. Reconstructing the continuum-cluster distribution function with four moments allows one to model dispersion, skewness, and kurtosis in the distribution, features that are readily compared with the experimental measurements. Results are presented for two values of the transition cluster size, $X_c = 2$ and 5, and three values of the growth exponent, $r = 0$, $\frac{1}{3}$, and $\frac{1}{2}$.

Figure 1 displays a comparison between the ME solution, denoted by symbols, with the corresponding FP approximation, shown with lines. The comparison is made for the toal cluster density using $r = \frac{1}{3}$ (Fig. 1a), and the average cluster size with $r = \frac{1}{2}$ (Fig. 1b). Compared to the ME solution, the FP approximation tends to overestimate the total cluster density and underestimate the average cluster size; however, the overall agreement appears very good. Since our clustering model focuses on single-atom transitions, a better agreement is found with $X_c = 5$ rather than $X_c = 2$ because the order of the transition (i.e., $\Delta = 1$) is closer to the neighborhood of $X_c = 2$, making these results more sensitive to transition-induced fluctuations. This demonstrates that the FP solution becomes a better

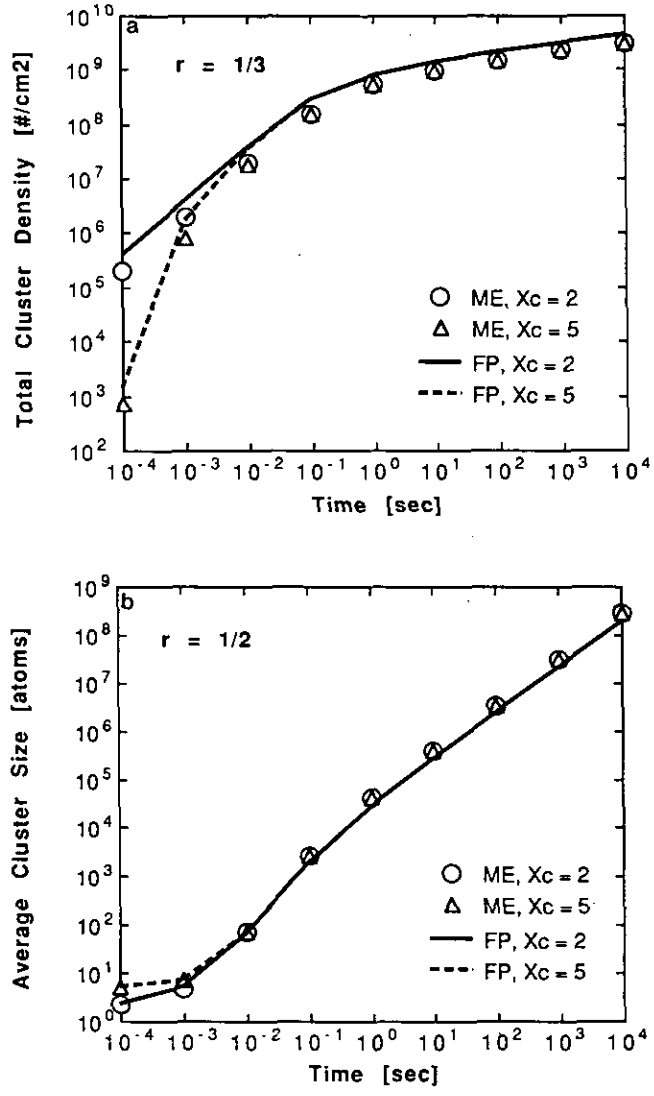

FIG. 1. Comparing characteristics of the continuum-cluster size distribution, computed from both the FP approximation and the corresponding ME solution: (a) total cluster density for $r = \frac{1}{3}$; (b) average cluster size for $r = \frac{1}{2}$.

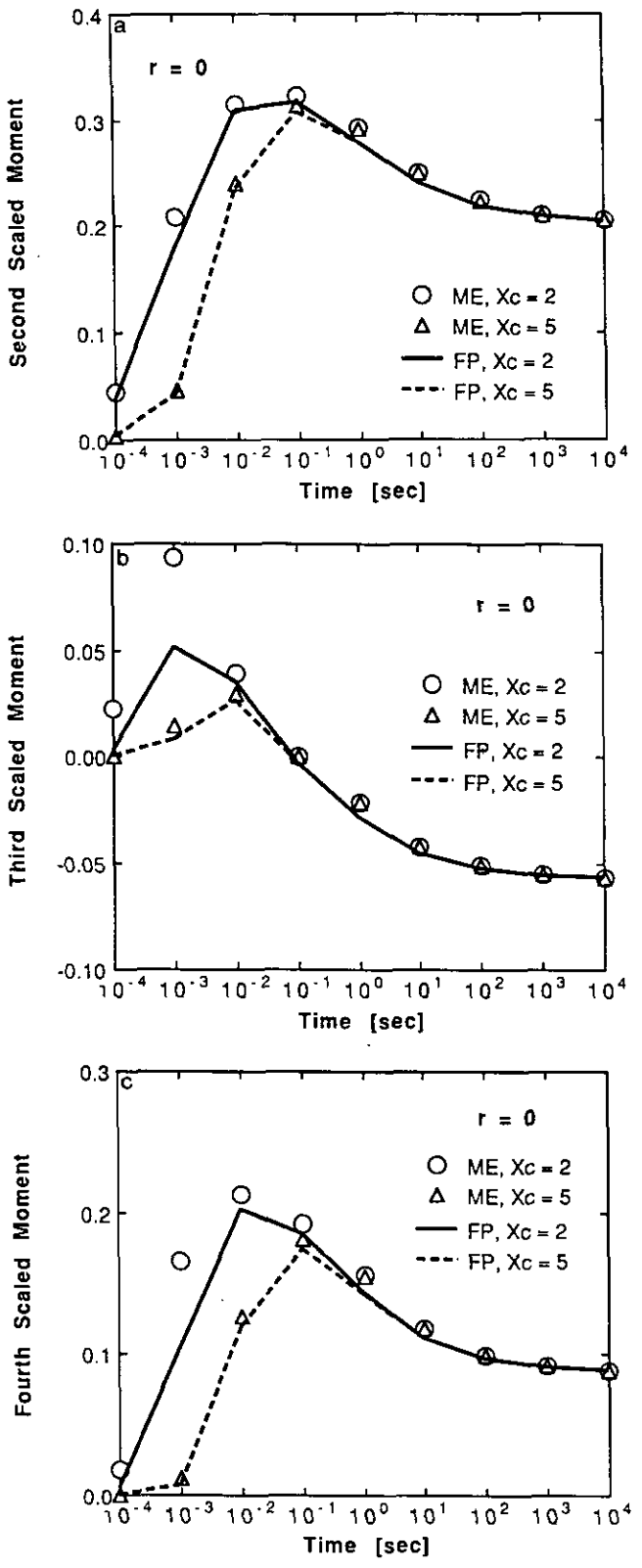

FIG. 2. Characteristics of the continuum-cluster size distribution, computed from both the FP approximation and the corresponding ME solution, for $r = 0$: (a) second scaled moment; (b) third scaled moment; (c) fourth scaled moment.

approximation to the ME solution when the transition size, Δ, is small in comparison to the size of the state at which the transition occurs (i.e., X_c).

During the early stages of the deposition process (i.e., for times $t < 10^{-2}$ s), the effect of increasing the transition size from $X_c = 2$ to $X_c = 5$ is seen as a general reduction in the total cluster density (Fig. 1a) with a corresponding increase in the average cluster size (Fig. 1b). This occurs because the $X_c = 5$ results consider 2, 3, and 4-atom clusters to be members of the discrete, small-size cluster population, whereas the $X_c = 2$ results place these clusters in the continuum group. Increasing X_c distributes more clusters in the discrete, small-size cluster group, hence decreasing the total density of *continuum* clusters (Fig. 1a), but increasing their average size (Fig. 1b). When the total cluster density and average size are considered for the *complete distribution* (which considers *both* the discrete, small-size clusters and the continuum, large-size population), these early clustering results do not depend on the choice of X_c [27]. At times later than 10^{-2} s, Fig. 1 indicates that this transition-size offset is eliminated because the average cluster size is much greater than X_c.

Figures 1a and b are indicative of the general trends for various growth exponents, r. Making allowance for variations in r produces only a quantitative change in the clustering results. More detailed analyses of the effects of cluster size-dependent aggregation and cluster geometry during the early stages of thin film formation can be found in Refs. [25, 27].

Figure 2 illustrates the moments of the continuum-cluster size distribution computed from both the ME solution (symbols) and FP approximation (lines). Results are presented for $r = 0$. Calculations using $r = \frac{1}{3}$ and $\frac{1}{2}$ show similar trends. The FP approximation underestimates the ME solution, most noticeably at the time of 10^{-3} s. Overall, the agreement between the two solution techniques is fairly good. As previously discussed, the $X_c = 5$ results compare better than the $X_c = 2$ results because the $X_c = 5$ calculations are less sensitive to transition-induced fluctuations. The offset displayed between the $X_c = 2$ and $X_c = 5$ results for times $t < 10^{-2}$ s is due to the fact that the moments shown in Fig. 2 are characteristic of the *continuum*-cluster size distribution; when moments are computed for the *complete* distribution, this discrepancy decreases significantly but is not eliminated. This may indicate that the cluster nucleation kinetics are more sensitive to the continuum properties of the complete distribution, rather than its discrete characteristics [27].

4. CONCLUSIONS

Our numerical analysis of the early stages of thin film formation indicate that a FP solution is a good approximation

to the corresponding ME approach. In the framework of a two-group model, in which clusters are placed into a discrete, small-size group or a continuum, large-size population, the FP approximation does surprisingly well down to $X_c = 2$ when only single-atom transitions govern the clustering kinetics. This may not be the case when cluster coalescence, dissociation events, or atom trapping at surface defects are included. Large-scale transitions, such as coalescence reactions, are best described by a two-group ME solution [23]. The influence of the transition cluster size, X_c, and the growth exponent, r, appears to be secondary to the effects of the expansion methods and moment evaluation techniques used in the ME and FP approaches. Although one may use the calculated moments to reconstruct the cluster distribution function, this reconstruction remains a separate problem and is not related to either the ME or the FP solution [23]. Consequently, it is more sensible to base numerical comparisons on moment calculations, as outlined in this paper.

REFERENCES

1. G. Nicolis and I. Prigogine, *Self-Organization in Nonequilibrium Systems: From Dissipative Structures to Order through Fluctuations* (Wiley, New York, 1977), Chap. 10.
2. G. Nicolis and A. Babloyantz, *J. Chem. Phys.* **51**, 2632 (1969).
3. E. O. Wilson, *The Insect Societies* (Harvard Univ. Press, Cambridge, MA, 1971), Chap. 21.
4. I. Prigogine and R. Herman, *Kinetic Theory of Vehicular Traffic* (American Elsevier, New York, 1971).
5. M. V. Smoluchowski, *Ann. Phys.* **21**, 756 (1906).
6. S. Chapman, *Phil. Trans. R. Soc. London A* **216**, 279 (1916).
7. A. Kolmogoroff, *Math. Ann.* **104**, 451 (1931).
8. I. Oppenheim, K. E. Shuler, and G. H. Weis, *Adv. Mol. Relax. Processes* **1**, 13 (1967–1968).
9. S. Chandrasekhar, *Rev. Mod. Phys.* **15**, 1 (1943).
10. H. A. Kramers, *Physica* **7**, 284 (1940).
11. J. E. Moyal, *J. R. Stat. Soc. B* **11**, 150 (1949).
12. L. M. Brown, A. Kelly, and R. M. Mayer, *Philos. Mag.* **19**, 721 (1969).
13. N. M. Ghoniem and D. D. Cho, *Phys. Status. Solidi A* **54**, 171 (1979).
14. G. Zinsmeister, *Thin Solid Films* **2**, 497 (1968).
15. J. A. Venables, *Philos. Mag.* **27**, 697 (1973).
16. J. B. Adams and W. N. G. Hitchon, *J. Comput. Phys.* **76**, 159 (1988).
17. C. A. Stone and N. M. Ghoniem, *J. Vac. Sci. Technol. A* **9** (3), 759 (1992).
18. N. M. Ghoniem and S. Sharafat, *J. Nucl. Mater.* **92**, 121 (1980).
19. S. Sharafat and N. M. Ghoniem, *Radiat. Eff. Def. Solids* **113**, 331 (1990).
20. M. Kiritani, *J. Phys. Soc. Jpn.* **35**, 95 (1973).
21. M. R. Hayns, *J. Nucl. Mater.* **59**, 175 (1976).
22. N. M. Ghoniem, *Phys. Rev. B* **39**, 11810 (1989).
23. M. Vicanek and N. M. Ghoniem, *J. Comput. Phys.* **101** (1), 1 (1992).
24. M. Vicanek, UCLA/ENG-9025, PPG-1321, University of California, Los Angeles, August 1990 (unpublished).
25. C. A. Stone and N. M. Ghoniem, *Vacuum* **41**, 1111 (1990).
26. G. Zinsmeister, *Vacuum* **16**, 529 (1966).
27. C. A. Stone, Ph.D. dissertation, University of California, Los Angeles, 1990.
28. F. Reif, *Fundamentals of Statistical and Thermophysics* (McGraw–Hill, New York, 1965), Chap. 15.